Ash from the Eyjafjallajokull eruption (Iceland): Fragmentation processes and aerodynamic behavior

Ash from the Eyjafjallajökull eruption (Iceland): Fragmentation processes and aerodynamic behavior

P. Dellino,[1] M. T. Gudmundsson,[2] G. Larsen,[2] D. Mele,[1] J. A. Stevenson,[3] T. Thordarson,[3] and B. Zimanowski[4]

Received 28 July 2011; revised 21 October 2011; accepted 25 October 2011; published 4 January 2012.

[1] The fragmentation process and aerodynamic behavior of ash from the Eyjafjallajökull eruption of 2010 are investigated by combining grain-size, Scanning Electron Microscopy (SEM), and quantitative particle morphology. Ash samples were collected on land in Iceland at 3–55 km distance from the volcanic vent, and represent various phases of the pulsating eruption. The grain size is fine even for deposits close to the vent, suggesting that the parent particle population at fragmentation consisted of a substantial amount of fine ash. SEM investigation reveals that ash produced during the first phase of the eruption consists of juvenile glass particles showing key features of magma-water interaction, suggesting that phreatomagmatism played a major role in the fragmentation of a vesicle-poor magma. In the last phase of the eruption, fragmentation was purely magmatic and resulted from stress-induced reaction of a microvesicular, fragile melt. The shape of ash, as determined by quantitative morphology analysis, is highly irregular, rendering the settling velocity quite low. This makes transportation by wind much easier than for other more regularly shaped particles of sedimentary origin. We conclude that the combination of magma's fine brittle fragmentation and irregular particle shape was the main factor in the extensive atmospheric circulation of ash from the mildly energetic Eyjafjallajökull eruption.

Citation: Dellino, P., M. T. Gudmundsson, G. Larsen, D. Mele, J. A. Stevenson, T. Thordarson, and B. Zimanowski (2012), Ash from the Eyjafjallajökull eruption (Iceland): Fragmentation processes and aerodynamic behavior, *J. Geophys. Res.*, *117*, B00C04, doi:10.1029/2011JB008726.

1. Introduction

[2] It is common knowledge in volcanology that Plinian eruptions [*Walker*, 1980; *Carey and Sparks*, 1986; *Carey and Sigurdsson*, 1989; *Bursik et al.*, 1992; *Sparks et al.*, 1991; *Fierstein and Nathenson*, 1992; *Sulpizio et al.*, 2008], which consist of more than 20-km high plumes transporting ash particles, can affect the atmosphere at a regional scale [*Folch et al.*, 2008; *Folch and Sulpizio*, 2010]. This type of volcanic eruption has been carefully monitored worldwide by air traffic authorities in the last decades [*Mastin et al.*, 2009; *Guffanti et al.*, 2010]. The Eyjafjallajökull eruption in Iceland in April–May 2010 was of a much smaller scale, yet ash atmospheric circulation caused turmoil in the air traffic corridors over Europe and North America for almost a month [*Schumann et al.*, 2011; M. T. Gudmundsson et al., Ash generation and distribution from the April–May 2010 eruption of Eyjafjallajökull, Iceland, submitted to *Earth and Planetary Science Letters*, 2011]. The eruption was pulsatory, consisting of many closely timed explosions, each releasing small parcels of ash, and was a long lasting one when compared to Plinian events [*Carey and Sigurdsson*, 1989]. The plume never exceeded an altitude of 10 km, and the mass flow rate of solid particles at the vent never exceeded 10^6 kg/s, which is an order of magnitude smaller than Plinian events [*Christiansen and Peterson*, 1981; *Sigurdsson et al.*, 1985; *Paladio-Melosantos et al.*, 1996]. The cumulative volume of particles emitted as tephra into the atmosphere over the entire eruption is estimated as 270 million m^3 (Gudmundsson et al., submitted manuscript, 2011), while in Plinian events order of magnitude larger volumes may be erupted in less than a day. Thus, given today's aircraft vulnerability to volcanic ash [*Blong*, 1984; *Casadevall*, 1993, 1994; *Miller and Casadevall*, 2000], even moderately sized eruptions can have severe effects when very fine ash, as produced during the Eyjafjallajökull eruption, enters atmosphere.

[3] Two basic questions need to be addressed in order to understand the mechanisms allowing the wide atmospheric dispersion of ash from the mildly energetic eruption of Eyjafjallajökull: (1) What was the melt fragmentation process that produced such fine-grained material? and (2) Why were ash particles so extensively transported in the atmosphere?

[1]Centro Interdipartimentale di Ricerca sul Rischio Sismico e Vulcanico, Dipartimento di Scienze della Terra e Geoambientali, Università di Bari, Bari, Italy.
[2]Institute of Earth Sciences, University of Iceland, Reykjavik, Iceland.
[3]School of Geosciences, University of Edinburgh, Edinburgh, UK.
[4]Physicalisch Vulkanologisches Labor, Universitaat Würzburg, Würzburg, Germany.

0148-0227/12/2011JB008726

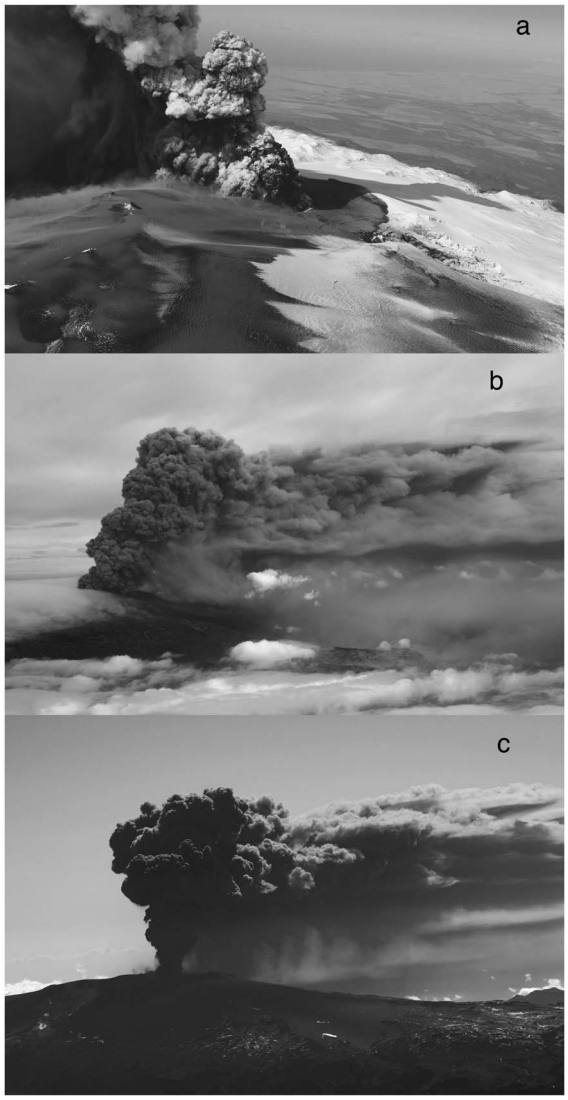

Figure 1. (a) Steam and tephra laden plume rising from the summit crater of Eyjafjallajökull on April 17, 2010. Minor base surges occurred frequently. (b) A weak plume rising to ~3.5 km elevation (2 km over vent) on April 27. (c) A "dry" plume at 4.5 km elevation (3 km over vent) on May 11. All photos courtesy of M. T. Gudmundsson.

[4] 1. In volcanic settings that host significant aquifers, it is important to determine whether effective magma-water interaction [*Wohletz*, 1983; *Heiken and Wohletz*, 1985; *Dellino and La Volpe*, 1995; *Büttner et al.*, 1999; *Stevenson et al.*, 2009], which is thought to produce fine-ash particles, played a role in the eruption dynamics, or whether magma fragmentation happened solely by magmatic processes.

[5] Magma-water interactions play an important role in fragmentation during subglacial eruptions. In basaltic, tuya-forming eruptions, phreatomagmatic fragmentation produces hyaloclastite and tephra in explosions that stop when water loses access to the vent [*Smellie*, 2000]. Fragmentation during subglacial eruptions of intermediate magma can be also phreatomagmatic, as was the case of the long-lived central volcano of Kerlingarfjöll in Iceland [*Stevenson et al.*, 2009]. Eruptions of more evolved magmas are more likely to be explosive irrespective of contact with water. Fragmentation during Quaternary subglacial rhyolite eruptions at Kerlingarfjöll was initially dominated by phreatomagmatic processes, but changed to magmatic processes as water lost access to the vent [*Stevenson et al.*, 2011]. In some cases, the presence of water can enhance fragmentation of an erupting magma foam, resulting in a phreatoplinian eruption (e.g., Askja, 1875 [*Carey et al.*, 2009]).

[6] The Eyjafjallajökull eruption experienced various phases, and likely different eruptive dynamics during its evolution. After an initial event of fire fountaining and lava flow occurring on the northeast flank of Eyjafjallajökull, in the ice-free area of Fimmvörðuháls between the ice caps of Eyjafjallajökull and Mýrdalsjökull (March 20-April 12), the eruption shifted to explosive activity at the summit caldera of Eyjafjallajökull. This explosive eruption lasted for 39 days, with the first explosive phase of about four days being the most intense and forming a plume rich in water vapor (Figure 1a). The second phase (April 18-May 4) of explosive activity was much weaker, and still some water vapor was visible in the plume (Figure 1b). During the third phase (approximately May 5- May 22), discharge rate and explosive activity increased again. Even though water may have had some access to the vent, the plume, which episodically reached above 6 km height, did not show signs of being enhanced by water vapor (Figure 1c). Summing up, the eruption showed signs of both a water-involved phase and of an effectively water-free phase, and fine ash was produced during all phases of the eruption. A correlation was observed between pyroclast size and magma discharge (Gudmundsson et al., submitted manuscript, 2011) through the eruption.

[7] 2. The distance that a falling particle can be carried depends on wind intensity and on the particle's aerodynamic behavior, in particular the terminal velocity, w (also called "settling velocity"). When particle terminal velocity is smaller than the turbulent shear velocity of a fluid current, dense solid particles are held in suspension and transported more easily by the current [*Dellino et al.*, 2008]. The turbulent shear velocity of a current is directly proportional to the time-averaged velocity of the current, thus, the lower the terminal velocity, the farther particles can be transported by a wind current [*Costa et al.*, 2006]. Particle's terminal velocity is defined by

$$w = \sqrt{\frac{4gd\left(\rho_s - \rho_f\right)}{3C_d\rho_f}} \tag{1}$$

with g, gravity acceleration, d particle size, ρ_s and ρ_f particle and fluid densities and C_d particle's drag coefficient.

[8] Equation (1) is the general form of terminal velocity, the so-called Newton impact law, and is valid for the whole range of particles' Reynolds numbers [*Middleton and Southard*, 1984], Re_p

$$\mathrm{Re}_p = \frac{\rho_f w d}{\mu} \tag{2}$$

with μ, fluid viscosity.

[9] Equation (1) shows that terminal velocity is not only a function of size and particle density but also of drag coefficient. The drag coefficient depends on Re_p and particle

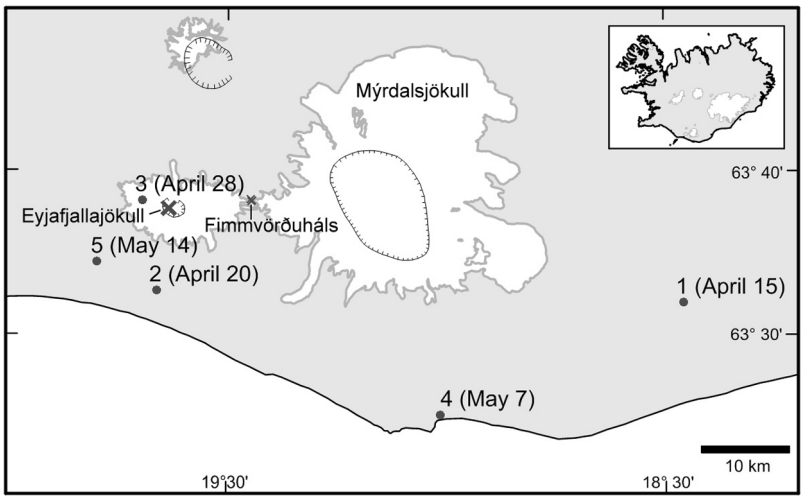

Figure 2. Location map. Sample location and date of sampling are marked. The cross marks the vent of the explosive eruption.

shape [*Walker et al.*, 1971; *Wilson and Huang*, 1979; *Arastoopour et al.*, 1982; *Suzuki*, 1983; *Ganser*, 1993; *Chhabra et al.*, 1999]. Spherical particles have a lower C_d and a higher settling velocity, while irregularly shaped particles of the same size have a higher C_d, hence fall more slowly, and more easily carried away by wind.

[10] To address particle origin and terminal velocity, in this paper we characterize magma fragmentation and ash particle aerodynamic characteristics of the various phases of the Eyjafjallajökull eruption, by combining grain-size analyses, SEM investigation and quantitative particle shape analysis.

2. Sample Description

[11] Ash samples were collected at various distances from the vent on land in Iceland, and represent the various phases of explosive activity. Sample locations and dates of collection are shown in Figure 2. Sample 1 is from the first phase of the eruption, and represents the climactic event of the first day, with the vapor-rich plume reaching a height of $\sim$10 km and a mass eruption rate of $\sim 10^6$ kg s^{-1}. Sample 2 is ash that fell on April 20, and belongs to the transition between the first and the second phase, with plume height much lower than on April 15 and mass eruption rate $< 10^4$ kg/s. Sample 3 is from the second phase of the eruption, when discharge of the explosive eruption was also low. Sample 4 is from the third phase of activity (discharge 10^5 kg/s) when the dry plume was reinvigorating, and reached a height of over 6 km. Sample 5 is also from the third phase of the eruption, and collected during the last several days of significant explosive activity. After May 17, an abrupt decline was recorded, and continuous explosive activity ceased on May 23 (Gudmundsson et al., submitted manuscript, 2011).

3. Grain Size Analyses

3.1. Method

[12] Grain-size analyses were carried out using a multimethod approach. The size fraction coarser than 3 ϕ (125 μm) was analyzed by means of standard sieves at half ϕ intervals, with $\phi = -log_2 d$, where d is diameter in mm. The fraction finer than 2 ϕ was analyzed by means of a Coulter Multisizer. Data from the two methods were matched by comparing the overlapping size classes (between 2 and 3 ϕ) and data were represented as weight percent at half-ϕ intervals (Figure 3). The cumulative curves are also shown in order to appreciate the total amount of fine ash present (>4 ϕ). The Median diameter, Md_ϕ = 50*th percentile*, and sorting, σ_ϕ = (84*th percentile* – 16*th percentile)*/2, as representative of the central tendency and of the dispersion statistics [*Inman*, 1952], are also shown.

3.2. Results and Interpretation

[13] All samples are fine grained, with the median size always finer than 1 mm, and lapilli never exceed a few percent of the total, even in the most proximal sample. At 10 km from the vent, a size fraction smaller than 16 μm (6 ϕ) starts to be significant, and it is quite abundant at 39 and 55 km, representing more than 20% of the total. As we are dealing with the material deposited on land (and hence more proximal to the vent), it is reasonable to assume that ash suspended in the atmosphere would have been still finer, revealing that the Eyjafjallajökull eruption resulted in a very fine parent grain size at fragmentation. Sorting is good (<2 ϕ), being lower for the three more proximal samples, and higher at larger distance, due to the presence of a bimodal distribution, with one mode centered on medium ash and the other on very fine ash. A good sorting is expected for fall deposits, and in the case of our bimodal distributions, the relatively higher value may be due both to the presence of ash aggregates [*Gilbert and Lane*, 1994; *Veitch and Woods*, 2001; *Wiesner et al.*, 2004] and to the fact that samples probably included ash from multiple thin laminae representing the sum of coarse and fine material deposited during eruption pulses. The very fine ash mode is present both in the sample from the "wet" phase of the eruption (sample 1 in Figure 2) and in the sample from the "dry" one (sample 4 in Figure 2), meaning that

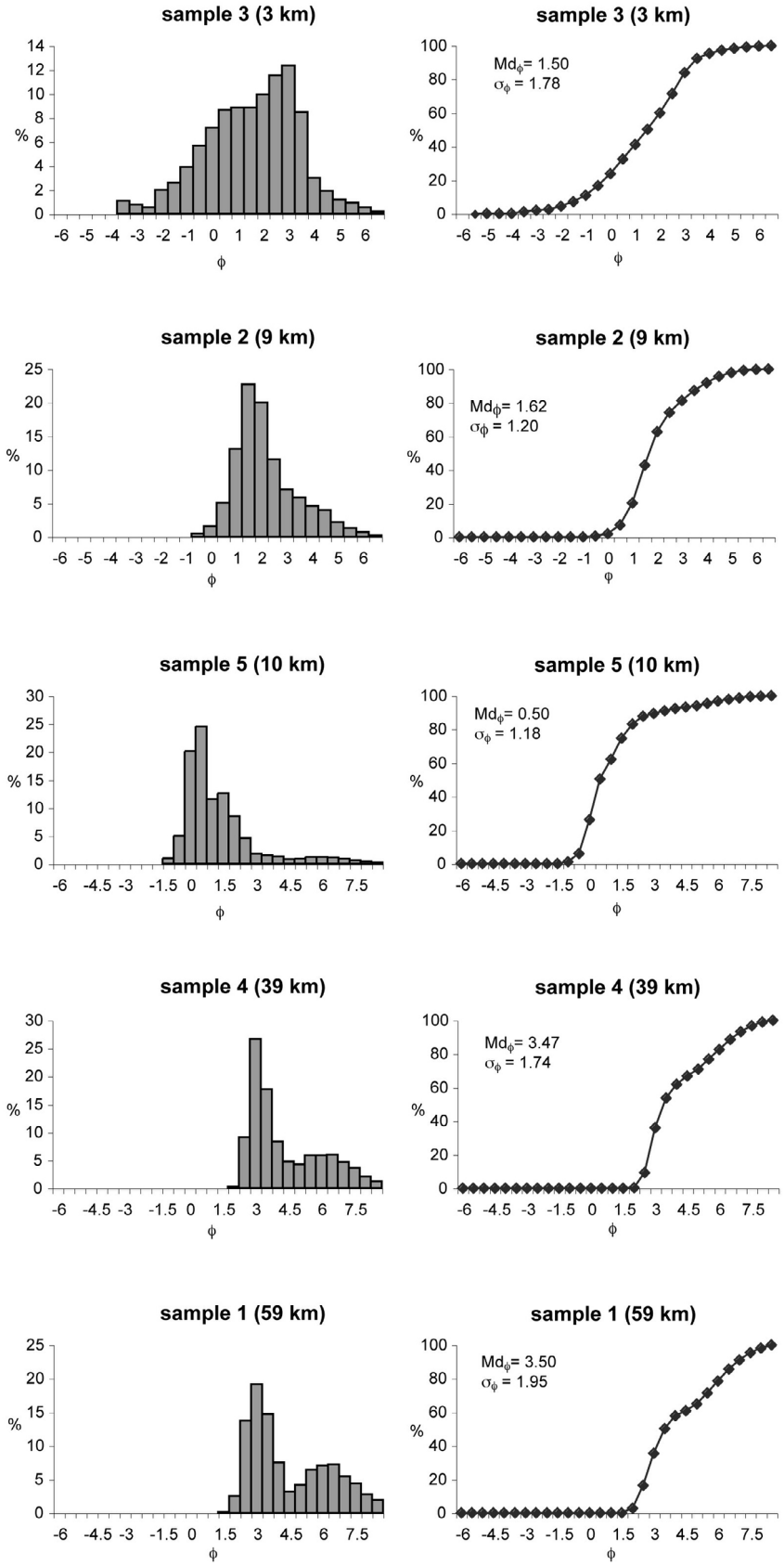

Figure 3. Montage showing (left) grain-size histograms and (right) cumulative distribution of the analyzed samples. Sample number is the same as Figure 2. In the insets the median size and sorting values are reported. Samples are ordered by increasing distance from the vent.

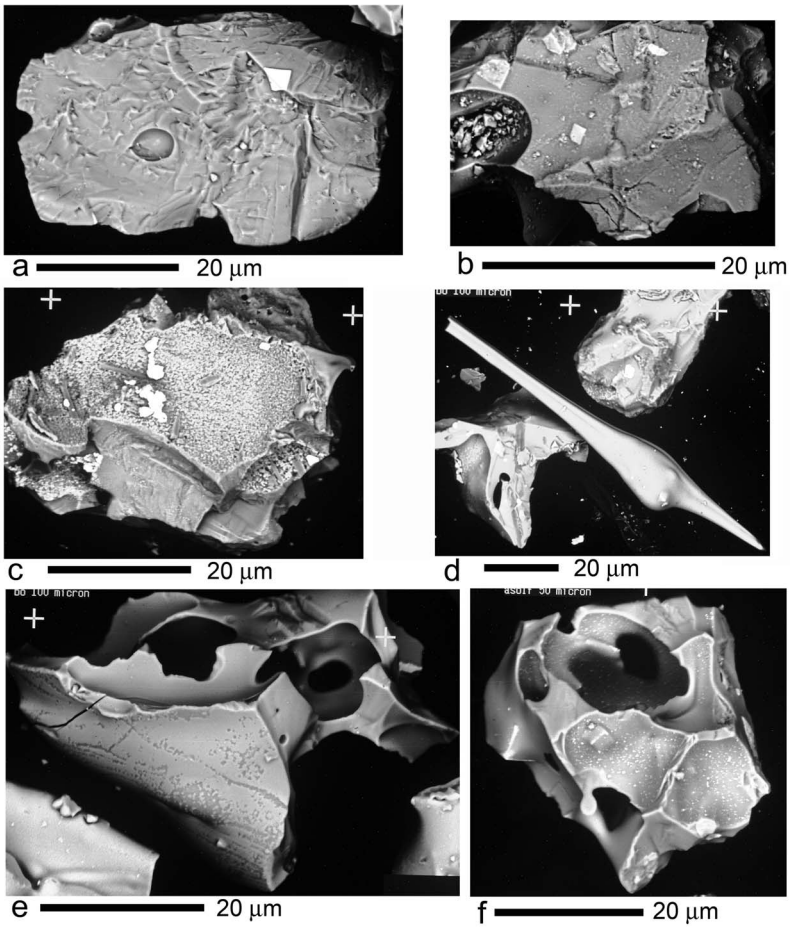

Figure 4. Montage showing a selection of representative ash particles at the SEM: (a) a blocky particle with stepped features, (b) an angular clast with quenching cracks, (c) an angular clast with a pitted surface, (d) a pelee's hair at the center and a moderately vesicular clast on the left, (e) a highly vesicular particle of irregular shape, and (f) a highly vesicular particle of angular shape.

fragmentation was very fine both for the "wet" plume and for the "dry" one.

4. SEM Investigation and Fragmentation Processes

4.1. Method

[14] SEM is a standard technique for investigating the fragmentation processes of explosive eruptions [*Heiken and Wohletz*, 1985]. It is based on the occurrence of key features on the vitric particle's surfaces [*Büttner et al.*, 1999; *Dellino and La Volpe*, 1995]. SEM images are here interpreted according to the classificatory schemes of previous studies in which particle coming from natural deposits were compared with those obtained by controlled laboratory experiments on magma fragmentation [*Büttner et al.*, 1999, 2002, 2006; *Dellino et al.*, 2001].

[15] In particular, we investigated the 4ϕ size fraction, because it is the one that best allows distinction between phreatomagmatic and magmatic fragmentation processes [*Dellino and La Volpe*, 1995]. SEM investigation was assisted by Energy Dispersive System (EDS) microanalyses, which allowed the characterization of glass surface composition. This confirmed that, during the explosive phase, a relatively evolved magma was involved and also allowed the identification of possible alteration processes, and the identification of lithic material resulting from fragmentation of the conduit walls. The amount of lithic clasts is very small (<5%), suggesting that fragmentation involved mostly magma. This could possibly be due to the fact that, in the later phases, the conduit was well established and the fragmentation did not cause any additional significant breakup of the conduit. It should be noted, however, that our data do not include any proximal samples. Observations show that large lithic blocks are found around the craters but volumetrically they represent only a small amount of the material in the proximal region. The low lithic content suggests that fragmentation took place at the interface between the melt and glacier ice, and occurred near the top of an open conduit rather than deeper in the conduit/dyke system.

4.2. Results and Interpretation

[16] Glassy ash from sample 1, representing the first day of the eruption when the highest plume, rich in water vapor, was formed, shows vesicle-poor clasts with the typical morphology of "interactive" particles produced during effective magma-water interaction: a blocky shape with stepped features due to intensive brittle magma fragmentation occurring at direct contact with water (Figure 4a) [*Büttner et al.*, 1999,

2002; *Dellino et al.*, 2001]. Sometimes the fracture pattern of the glass surface, which formed because of particle contraction due to rapid quenching upon fast acceleration in contact with water, is visible (Figure 4b) [*Büttner et al.*, 1999, 2002; *Dellino et al.*, 2001].

[17] Particles coming from sample 3 represent the phase of the eruption at the end of April when water was still in contact with the melt in the shallow conduit, resulting in magma-water interaction that formed the typical pitted surface of phreatomagmatic clasts (Figure 4c) [*Büttner et al.*, 2002]. Also Pelee's hair clasts are present (Figure 4d) and could represent ductile fragmentation of a low viscosity melt, which was triggered by the decompression of the magma-water explosion. This kind of clast is commonly reported from basaltic environments, often associated with littoral or rootless cones as well [e.g., *Kauahikaua et al.*, 2003]. In Figure 4d a moderately vesicular particle is also present, suggesting that gas exsolution processes and gas bubble formation were active during this phase of the eruption.

[18] Samples 4 and 5, representing the dry-plume phase of the eruption, consist mostly of highly vesicular clasts, and do not show any features related to magma-water interaction. Clast morphology is angular/irregular (Figure 4e), with the contours representing septa of small broken gas bubbles (Figure 4f). These features suggest that, during the final phase of the eruption, a batch of microvesicular magma was involved, which reacted to the shear stress induced during flow through the conduit with brittle fragmentation [*Büttner et al.*, 2002, 2006; *Gardner et al.*, 1996]. In this case it seems that magma-water interaction did not contribute substantially to fragmentation.

[19] Summing up, it is possible to suggest that the most energetic initial phase of the eruption, which formed a plume rich in water vapor generated by magma-water interaction, was characterized by phreatomagmatic explosions that favored fragmentation of a vesicle-poor magma into fine ash. Magma-water interaction was significant also during the second week of the eruption, while it declined at the end of the eruption, probably because magma, though still flowing in the conduit, did not come into effective contact with ice-meltwater. During this phase, meltwater was drained out of the glacier as jökulhaups that went to north. Also during the water-free final phase of the eruption, which was punctuated by periodic resurgences of explosive activity, fine ash was formed. In this case, it was probably the very fragile nature of magma, due to high microvesicularity, that favored brittle-type magmatic fine ash fragmentation [*Zimanowski et al.*, 2003; *Büttner et al.*, 2006]. The Eyjafjallajökull eruption was therefore characterized by both phreatomagmatic and magmatic fragmentation pulses, both of which produced fine ash. Thus, irrespective of the type of fragmentation that dictated the formation of fine particles, during both magma-water interaction and magmatic episodes, intensive brittle fragmentation occurred, which is a major factor in the formation of fine ash [*Papale*, 1999; *Zimanowski et al.*, 2003; *Büttner et al.*, 2006; *Gonnermann and Manga*, 2003].

5. Quantitative Particle Morphology Analyses and Aerodynamic Behavior

5.1. Method

[20] As the aerodynamic behavior of ash is determined by terminal velocity, and since terminal velocity is influenced by the drag coefficient, which in turn is dependent both on particle Reynolds number and shape, a model that takes particle shape into account is needed. We used the experimental model of *Dellino et al.* [2005], which is able to predict the drag coefficient (C_d) of particles by means of the shape factor, Ψ

$$C_d = \frac{0.69 g {d_{sph}}^3 \rho_f \left(1.33\rho_s - 1.33\rho_f\right)}{\mu^2 \left(\frac{g\Psi^{1.6} {d_{sph}}^3 \rho_f \left(\rho_s - \rho_f\right)}{\mu^2}\right)^{1.0412}} \quad (3)$$

with d_{sph} diameter of the sphere equivalent in volume to the particle. Equation (3) returns C_d values with a good approximation, in a range of particle Reynolds numbers between 2×10^5 and 5×10 [*Mele et al.*, 2011a]. In order to determine the shape factor, and particle density, we carried out quantitative particle morphology analysis, following the approach of *Dellino et al.* [2005, 2008] and *Mele et al.* [2011a]. The size fraction between 2 and 3 ϕ (125–250 μm) was chosen. Its shape was considered as representative also of that of finer particles, since pyroclasts particles finer than 3ϕ have generally a shape factor similar to that of the 2–3 ϕ fraction [*Mele et al.*, 2011a].

[21] Particle density was measured using a standard Gay Lussac picnometer of 5 ml capacity. Because of the small grain size, we selected ~0.2 g of particles for each sample, and calculated the average value. The density is ~2200 kg m^3 for the magmatic particles, and ~2500 kg m^3 for the phreatomagmatic particles. Since pyroclastic particles are not spherical, the actual grain size does not match the sieves grain size. This is because sieves sort grains by their intermediate and smallest axes. Therefore, the sieve mesh describes only a bidimensional measure of particles [*Sahu*, 1965; *Baba and Komar*, 1981]. In order to obtain a tridimensional measure, we used the diameter of the equivalent sphere, d_{sph}, by means of:

$$d_{sph} = \sqrt[3]{\frac{6m}{\pi\rho_s}} \quad (4)$$

Equation (4) takes into account particle volume, by considering the actual mass m and density, ρ_s, of particles. The mass, m, of particles was measured by picking at random 200 particles for each sample, and calculating the average mass.

[22] The shape factor, Ψ, is a dimensionless parameter describing particle shape and is defined as the ratio of sphericity, Φ, and circularity X [*Dellino et al.*, 2005, 2008]. Sphericity, Φ, is defined as the ratio A_{sph}/A_p, where A_{sph} is the surface area of the equivalent sphere and A_p is the particle's surface area.

[23] A_{sph} is equal to:

$$A_{sph} = 4\pi\left(\frac{d_{sph}}{2}\right)^2 \quad (5)$$

A_p can be approximated to a scalene ellipsoid, by means of

$$A_p = 4\pi\left(\frac{(D_l/2)^z(D_m/2)^z + (D_l/2)^z(D_s/2)^z + (D_m/2)^z(D_s/2)^z}{2}\right)^{1/z} \quad (6)$$

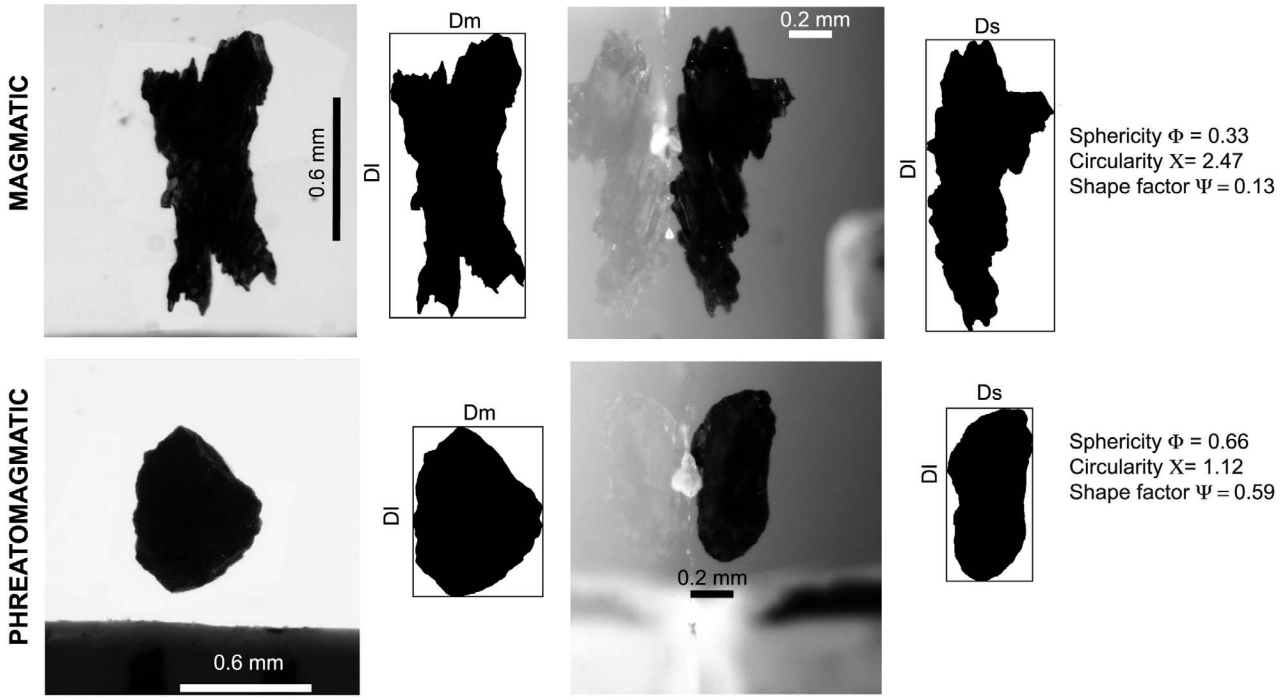

Figure 5. Montage showing (top) a magmatic particle and (bottom) a phreatomagmatic particle shot under a stereoscope equipped with a revolving table. The insets in Figure 5 (left) report the digital binarized silhouette used for image analysis. Each particle is shown by the two orientations used for measuring the three orthogonal particle axes. The insets in Figure 5 (right) report the morphology parameters and shape factor.

where D_l, D_m and D_s are the three particle axes, and $z = 1.6075$ (Knud Thomsen's formula).

[24] Circularity, X, is the ratio of the maximum projection perimeter P_{mp} and the perimeter of the circle equivalent to the maximum projection area, A_{mp} of a particle.

[25] The shape factor ranges between 0 and 1. A spherical particle has $\Psi = 1$. The lower Ψ values indicate more irregular particle shapes.

[26] In order to measure morphology, 60 particles coming from samples of the phreatomagmatic phase and 60 coming from the magmatic phase were picked at random from the whole particle population and mounted on a revolving table under a stereomicroscope. The method is fully explained by *Dellino et al.* [2005]. The three particle axes, and circularity, were measured by means of image-analysis techniques on high-resolution digital images. Each particle had a resolution of about 5000 pixels. Figure 5 shows an example of a particle from magmatic fragmentation and one from phreatomagmatic fragmentation, together with the silhouette obtained after image processing analysis. The shapes are quite different, with the magmatic particle being more irregular than the phreatomagmatic one. The irregularity of the magmatic particle's contour is due to the presence of septa between small broken vesicles.

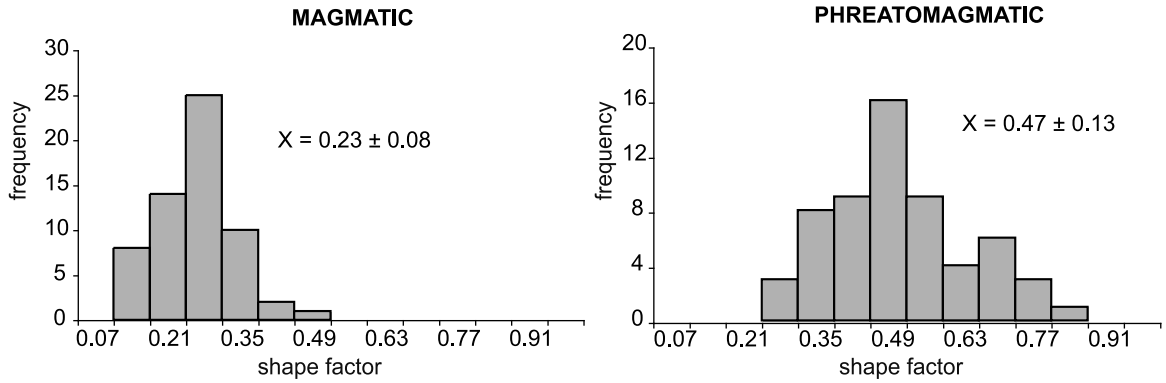

Figure 6. Histograms showing the distribution of shape factor values of (left) magmatic and (right) phreatomagmatic particles. The average value and the range of the standard deviation around the mean are also shown.

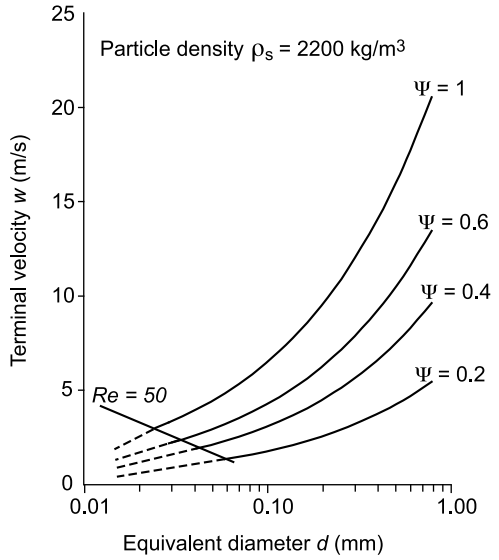

Figure 7. Diagram showing terminal velocity as a function of diameter for particles of 2200 kg m^3 density. The curves represent different values of shape factor. The dashed lines were drawn by extrapolation and represent values for particle at $Re_p < 50$.

5.2. Results

[27] In Figure 6, histograms show the distribution of the shape factor for magmatic and phreatomagmatic particles, together with the average value and standard deviation. The higher irregularity of magmatic particles makes their shape factor lower, with an average value of 0.23; while phreatomagmatic particles have an average value of 0.47. Both magmatic and phreatomagmatic particles have shape factor much smaller than that of spherical particles ($\Psi = 1$).

[28] With the measured values of particle density and shape factor, the settling velocity was calculated by combining equations (1) and (3). In the calculation, we used air as fluid, with a viscosity of 1.82×10^{-5} Pa s and density of 1.22 kg m^3.

[29] For illustrating the influence of size and shape on settling velocity, in Figure 7 it is shown how settling velocity changes as a function of size for different Ψ, including $\Psi = 1$ that represents spherical particles. A value of 2200 kg m^3 is used for particle density, as a representative value for moderately vesicular clasts. Magmatic particles settle more slowly than phreatomagmatic ones, and thus are held in suspension by wind even more easily. This could explain why, during the magmatic phase, which had a lower plume than the phreatomagmatic phase, fine particles were still transported in the atmosphere to mainland Europe, a distance of some 2000 km [e.g., *Schumann et al.*, 2011].

[30] The solid lines in Figure 7 refer to particles down to 4 ϕ, which correspond to $Re_p \sim 50$. Down to this value of Re_p, equation (3) approximates well the values of C_d. For $Re_p < 50$, equation (3) underestimates C_d, therefore overestimating settling velocity. However, by knowing the difference between values calculated by our method at $\Psi = 1$ versus the literature data for spherical particles, we can evaluate the underestimation of C_d for spherical particles at $Re_p < 50$. By assuming that particles with a lower Ψ define a $C_d - Re_p$ line parallel to spherical ones, but shifted toward higher C_d values [*Dellino et al.*, 2005], it is possible to extrapolate C_d to lower Re_p, and evaluate the overestimation of settling velocity. In Figure 7, the dotted lines are extrapolations of settling velocity down to grain size of 6 ϕ (16 μm), drawn by taking this underestimation into account. Clearly, an implementation of the model of *Dellino et al.* [2005], which can predict the C_d for very low Re_p would be helpful. For the present analysis, however, the extrapolation of Figure 7 provides an acceptable approximation of the settling velocity of very fine ash.

[31] By comparing the settling velocity of the irregularly shaped ash of the Eyjafjallajökull eruption with that of spheres ($\Psi = 1$), one can see that ash particles, falling much more slowly, are more easily transported in suspension by wind than are more regularly shaped particles, such as quartz sand and dust in a desert storm.

6. Summary and Conclusion

[32] The explosive activity of Eyjafjallajökull's 2010 eruption in Iceland was characterized by closely timed pulses resulting from discrete fragmentation events, each involving a small batch of magma. As the pulses recurred at short time-intervals, the plume was fed semi-continuously, which resulted in periodic changes of height related to variations in the mass eruption rate at the vent. The mass eruption rate never reached very high values when compared to plinian eruptions, and the plume height never exceeded 10 km. Nevertheless, the large amount of fine ash (a substantial proportion of it finer than 16 μm) produced at fragmentation, aided by the specific morphology of the particles, allowed long-distance transport and wide atmospheric circulation.

[33] During the first phase of the eruption, the plume was rich in water vapor, whereas it was dry during the final phase. SEM investigation shows that, during the first phase, effective magma-water interaction influenced fragmentation. This confirms the role of glacial meltwater in driving the explosions of the first phase. During the final phase, water was probably no longer in effective contact with the melt and fragmentation was purely magmatic. Anyway, despite the lack of magma-water interaction, as indicated by SEM investigation, continued brittle magma fragmentation allowed the production of fine ash, because the melt was microvesicular and thus highly fragile [*Büttner et al.*, 2006; *Rose and Durant*, 2009; *Mele et al.*, 2011b]. This means that fine ash can be produced in significant quantities both by phreatomagmatic and by magmatic processes. When dealing with brittle magma fragmentation, once the critical strain rate of fragmentation is overcome [*Büttner et al.*, 2006], it is the spall strength of the magma (fragility) that controls grain size, and this is particularly low for microvesicular magmas.

[34] The difference in settling velocity between the irregularly shaped ash of the Eyjafjallajökull eruption and equivalent spheres is up to ~400% (about 2 m s^{-1} for spheres of 16 μm versus about 0.5 m/s for irregularly shaped ash particles of the same size with $\Psi = 0.2$). The specific morphology of ash makes it much more easily held in suspension by wind compared to other sedimentary particles of more regular shape.

[35] **Acknowledgment.** Michael Ort, Karoly Nemeth, and an anonymous reviewer greatly helped in improving the manuscript.

References

Arastoopour, H., C. H. Wang, and S. A. Weil (1982), Particle–particle interaction in a dilute gas–solid system, *Chem. Eng. Sci.*, *37*, 1379–1386, doi:10.1016/0009-2509(82)85010-0.

Baba, J., and P. D. Komar (1981), Settling velocities of irregular grain at low Reynolds numbers, *J. Sediment. Petrol.*, *51*, 121–128.

Blong, R. J. (1984), *Volcanic Hazards: A Sourcebook on the Effects of Eruptions*, Academic, Sidney, Australia.

Bursik, M. I., R. S. J. Sparks, J. S. Gilbert, and S. N. Carey (1992), Sedimentation of tephra by volcanic plumes I. Theory and its comparison with a study of the Fogo A plinian deposits, Sao Miguel (Azores), *Bull. Volcanol.*, *54*, 329–344, doi:10.1007/BF00301486.

Büttner, R., P. Dellino, and B. Zimanowsky (1999), Identifying magma-water interaction from the surface features of ash particles, *Nature*, *401*, 688–690, doi:10.1038/44364.

Büttner, R., P. Dellino, L. La Volpe, V. Lorenz, and B. Zimanowsky (2002), Thermohydraulic explosions in phreatomagmatic eruptions as evidenced by the comparison between pyroclasts and products from Molten Fuel Interaction experiments, *J. Geophys. Res.*, *107*(B11), 2277, doi:10.1029/2001JB000511.

Büttner, R., P. Dellino, H. Raue, I. Sonder, and B. Zimanowski (2006), Stress induced brittle fragmentation of magmatic melts: Theory and experiments, *J. Geophys. Res.*, *111*, B08204, doi:10.1029/2005JB003958.

Carey, S. N., and H. Sigurdsson (1989), The intensity of Plinian eruptions, *Bull. Volcanol.*, *51*, 28–40, doi:10.1007/BF01086759.

Carey, S. N., and R. S. J. Sparks (1986), Quantitative models of fallout and dispersal of tephra from volcanic eruption columns, *Bull. Volcanol.*, *48*, 109–125, doi:10.1007/BF01046546.

Carey, R. J., B. F. Houghton, and T. Thordarson (2009), Abrupt shifts between wet and dry phases of the 1875 eruption of Askja Volcano: Microscopic evidence for macroscopic dynamics, *J. Volcanol. Geotherm. Res.*, *184*(3–4), 256–270, doi:10.1016/j.jvolgeores.2009.04.003.

Casadevall, T. J. (1993), Volcanic hazards and aviation safety, lessons of the past decade, *FAA Aviat. Saf. J.*, *2*, 1–11.

Casadevall, T. J. (Ed.) (1994), Volcanic ash and aviation safety. Proceedings of the First International Symposium on Volcanic Ash and Aviation Safety, *U.S. Geol. Surv. Bull.*, *2047*, 1–418.

Chhabra, R. P., L. Agarwal, and N. K. Sinha (1999), Drag on non-spherical particles: An evaluation of available methods, *Powder Technol.*, *101*, 288–295, doi:10.1016/S0032-5910(98)00178-8.

Christiansen, R. L., and D. W. Peterson (1981), Chronology of the 1980 eruptive activity, *U.S. Geol. Surv. Prof. Pap.*, *1250*, 17–30.

Costa, A., G. Macedonio, and A. Folch (2006), A three-dimensional Eulerian model for transport and deposition of volcanic ashes, *Earth Planet. Sci. Lett.*, *241*, 634–647, doi:10.1016/j.epsl.2005.11.019.

Dellino, P., and L. La Volpe (1995), Fragmentation versus transportation mechanisms in the pyroclastic sequence of Monte Pilato-Rocche Rosse (Lipari, Italy), *J. Volcanol. Geotherm. Res.*, *64*, 211–231, doi:10.1016/0377-0273(94)00084-T.

Dellino, P., R. Isaia, L. La Volpe, and G. Orsi (2001), Statistical analysis of textural data from complex pyroclastic sequence: Implication for fragmentation processes of the Agnano-Monte Spina eruption (4.1 ka), Phlegraean Fields, southern Italy, *Bull. Volcanol.*, *63*, 443–461, doi:10.1007/s004450100163.

Dellino, P., D. Mele, R. Bonasia, G. Braia, L. La Volpe, and R. Sulpizio (2005), The analysis of the influence of pumice shape on its terminal velocity, *Geophys. Res. Lett.*, *32*, L21306, doi:10.1029/2005GL023954.

Dellino, P., D. Mele, R. Sulpizio, L. La Volpe, and G. Braia (2008), A method for the calculation of the impact parameters of dilute pyroclastic density currents based on deposit particle characteristics, *J. Geophys. Res.*, *113*, B07206, doi:10.1029/2007JB005365.

Fierstein, J., and M. Nathenson (1992), Another look at the calculation of fallout tephra volumes, *Bull. Volcanol.*, *54*, 156–167, doi:10.1007/BF00278005.

Folch, A., and R. Sulpizio (2010), Evaluating long-range volcanic ash hazard using supercomputing facilities: Application to Somma-Vesuvius (Italy), and consequences for civil aviation over the Central Mediterranean Area, *Bull. Volcanol.*, *72*, 1039–1059, doi:10.1007/s00445-010-0386-3.

Folch, A., O. Jorba, and J. Viramonte (2008), Volcanic ash forecast—Application to the May 2008 Chaitén eruption, *Nat. Hazards Earth Syst. Sci.*, *8*, 927–940, doi:10.5194/nhess-8-927-2008.

Ganser, G. (1993), A rational approach to drag prediction of spherical and non-spherical particles, *Powder Technol.*, *77*, 143–152, doi:10.1016/0032-5910(93)80051-B.

Gardner, J. E., R. M. E. Thomas, C. Jaupart, and S. Tait (1996), Fragmentation of magma during Plinian volcanic eruptions, *Bull. Volcanol.*, *58*, 144–162, doi:10.1007/s004450050132.

Gilbert, J. S., and S. J. Lane (1994), The origin of accretionary lapilli, *Bull. Volcanol.*, *56*, 398–411.

Gonnermann, H. M., and M. Manga (2003), Explosive volcanism may not be an inevitable consequence of magma fragmentation, *Nature*, *426*, 432–435, doi:10.1038/nature02138.

Guffanti, M., D. J. Schneider, K. L. Wallace, T. Hall, D. R. Bensimon, and L. J. Salinas (2010), Aviation response to a widely dispersed ash and gas cloud from the August 2008 eruption of Kasotochi, Alaska, USA, *J. Geophys. Res.*, *115*, D00L19, doi:10.1029/2010JD013868.

Heiken, G., and K. Wohletz (1985), *Volcanic Ash*, 246 pp., Univ. of California Press, Berkeley.

Inman, D. L. (1952), Measures for describing the size-distribution of sediments, *J. Sediment. Res.*, *22*, 125–145.

Kauahikaua, J., D. R. Sherrod, K. V. Cashman, C. Heliker, K. Hon, T. N. Mattox, and J. A. Johnson (2003), Hawaiian lava-flow dynamics during the Pu'u 'Ō'ō-Kū paianaha eruption: A tale of two decades, *U.S. Geol. Surv. Prof. Pap.*, *1676*, 63–87.

Mastin, L. G., et al. (2009), A multidisciplinary effort to assign realistic source parameters to models of volcanic ash-cloud transport and dispersion during eruptions, *J. Volcanol. Geotherm. Res.*, *186*, 10–21, doi:10.1016/j.jvolgeores.2009.01.008.

Mele, D., P. Dellino, R. Sulpizio, and G. Braia (2011a), A systematic investigation on the aerodynamics of ash particles, *J. Volcanol. Geotherm. Res.*, *203*, 1–11, doi:10.1016/j.jvolgeores.2011.04.004.

Mele, D., R. Sulpizio, P. Dellino, and L. La Volpe (2011b), Stratigraphy and eruptive dynamics of a pulsating Plinian eruption of Somma-Vesuvius: The Pomici di Mercato, *Bull. Volcanol.*, *73*, 257–278, doi:10.1007/s00445-010-0407-2.

Middleton, G. V., and J. B. Southard (1984), *Mechanics of Sediment Movement, Soc*, 401 pp., Econ. Miner, Tulsa, Okla.

Miller, T. P., and T. J. Casadevall (2000), Volcanic ash hazards to aviation, in *Encyclopedia of Volcanoes*, edited by H. Sigurdsson et al., pp. 915–930, Academic, San Diego, Calif.

Paladio-Melosantos, M. L. O., R. U. Solidum, W. E. Scott, R. B. Quiambao, J. V. Umbal, K. S. Rodolfo, B. S. Tubianosa, P. J. Delos Reyes, R. A. Alonso, and H. B. Ruelo (1996), Tephra falls of the 1991 eruptions of Mount Pinatubo, in *Fire and Mud: Eruptions and Lahars of Mount Pinatubo, Philippines*, edited by C. G. Newhall and R. S. Punongbayan, pp. 687–731, Philipp. Inst. of Volcanol. and Seismol, Quezon City, Philippines.

Papale, P. (1999), Strain-induced fragmentation in explosive eruptions, *Nature*, *397*, 425–428, doi:10.1038/17109.

Rose, W. I., and A. J. Durant (2009), Fine ash content of explosive eruption, *J. Volcanol. Geotherm. Res.*, *186*, 32–39, doi:10.1016/j.jvolgeores.2009.01.010.

Sahu, B. K. (1965), Theory of sieving, *J. Sediment. Petrol.*, *35*, 750–753.

Schumann, U., et al. (2011), Airborne observations of the Eyjafjalla volcano ash cloud over Europe during air space closure in April and May 2010, *Atmos. Chem. Phys.*, *11*, 2245–2279, doi:10.5194/acp-11-2245-2011.

Sigurdsson, H., S. Carey, W. Cornell, and T. Pescatore (1985), The eruption of Vesuvius in AD 79, *Natl. Geogr. Res.*, *1*, 332–387.

Smellie, J. L. (2000), Subglacial eruptions, in *Encyclopedia of Volcanoes*, edited by H. Sigurdsson et al., pp. 403–418, Academic, London.

Sparks, R. S. J., S. N. Carey, and H. Sigurdsson (1991), Sedimentation from gravity currents generated by turbulent plumes, *Sedimentology*, *38*, 839–856, doi:10.1111/j.1365-3091.1991.tb01875.x.

Stevenson, J. A., J. L. Smellie, D. W. McGarvie, J. S. Gilbert, and B. I. Cameron (2009), Subglacial intermediate volcanism at Kerlingarfjöll, Iceland: Magma-water interactions beneath thick ice, *J. Volcanol. Geotherm. Res.*, *185*, 337–351, doi:10.1016/j.jvolgeores.2008.12.016.

Stevenson, J. A., J. S. Gilbert, D. W. McGarvie, and J. L. Smellie (2011), Explosive rhyolite tuya formation: Classic examples from Kerlingarfjöll, Iceland, *Quat. Sci. Rev.*, *30*(1–2), 192–209, doi:10.1016/j.quascirev.2010.10.011.

Sulpizio, R., R. Bonasia, P. Dellino, M. A. Di Vito, L. La Volpe, D. Mele, G. Zanchetta, and L. Sadori (2008), Discriminating the long distance dispersal of fine ash from sustained columns or near ground ash cloud: The example of the Pomici di Avellino eruption (Somma-Vesuvius, Italy), *J. Volcanol. Geotherm. Res.*, *177*, 263–276, doi:10.1016/j.jvolgeores.2007.11.012.

Suzuki, T. (1983), A theoretical model for dispersion of tephra, in *Arc Volcanism: Physics and Tectonics*, edited by D. Shimozuru and I. Yokoyama, pp. 95–113, Terra Sci., Tokyo.

Veitch, G., and A. W. Woods (2001), Particle aggregation in volcanic eruption columns, *J. Geophys. Res.*, *106*(B11), 26,425–26,441, doi:10.1029/2000JB900343.

Walker, G. P. L. (1980), The Taupo pumice: Product of the most powerful known (ultraplinian) eruption?, *J. Volcanol. Geotherm. Res.*, *8*, 69–94, doi:10.1016/0377-0273(80)90008-6.

Walker, G. P. L., L. Wilson, and E. L. G. Bowell (1971), Explosive volcanic eruptions: I. Rate of fall of pyroclasts, *Geophys. J. R. Astron. Soc.*, *22*, 377–383.

Wiesner, M. G., A. Wetzel, S. G. Catane, E. L. Listanco, and H. T. Mirabueno (2004), Grain size, areal thickness distribution and controls on sedimentation of the 1991 Mount Pinatubo tephra layer in the South China Sea, *Bull. Volcanol.*, *66*, 226–242, doi:10.1007/s00445-003-0306-x.

Wilson, L., and T. C. Huang (1979), The influence of shape on the atmospheric settling velocity of volcanic ash particles, *Earth Planet. Sci. Lett.*, *44*, 311–324, doi:10.1016/0012-821X(79)90179-1.

Wohletz, K. H. (1983), Mechanisms of hydrovolcanic pyroclast formation: Grain-size, scanning electron microscopy, and experimental studies, *J. Volcanol. Geotherm. Res.*, *17*, 31–63, doi:10.1016/0377-0273(83)90061-6.

Zimanowski, B., K. H. Wohletz, R. Büttner, and P. Dellino (2003), The volcanic ash problem, *J. Volcanol. Geotherm. Res.*, *122*, 1–5, doi:10.1016/S0377-0273(02)00471-7.

P. Dellino and D. Mele, Centro Interdipartimentale di Ricerca sul Rischio Sismico e Vulcanico, Dipartimento di Scienze della Terra e Geoambientali, Università di Bari, Via E. Orabona 4, I-70125 Bari, Italy. (dellino@geomin.uniba.it)

M. T. Gudmundsson and G. Larsen, Institute of Earth Sciences, University of Iceland, Sturlugata 7, IS-101 Reykjavik, Iceland.

J. A. Stevenson and T. Thordarson, School of Geosciences, University of Edinburgh, West Mains Rd., Edinburgh EH9 3JW, UK.

B. Zimanowski, Physicalisch Vulkanologisches Labor, Universitaat Würzburg, Pleicherwall 1, D-97070, Würzburg, Germany.